Absolute photoionization cross section measurements of the Kr I-isoelectronic sequence

D. Kilbane,[1] F. Folkmann,[2] J.-M. Bizau,[3] C. Banahan,[1] S. Scully,[4] H. Kjeldsen,[2]
P. van Kampen,[1] M. W. D. Mansfield,[5] J. T. Costello,[1] and J. B. West[6]

[1]NCPST and The School of Physical Sciences, Dublin City University, Ireland
[2]Institute of Physics and Astronomy, University of Aarhus, DK-8000 Aarhus C, Denmark
[3]LIXAM, Université Paris Sud, Orsay 91405, France
[4]School of Mathematics and Physics, Queen's University of Belfast, Belfast BT7 1NN, UK
[5]Department of Physics, University College Cork, Cork, Ireland
[6]Daresbury Laboratory, Warrington WA4 4AD, UK

Photoionization spectra have been recorded in the $4s$, $4p$ and $3d$ resonance regions for the Kr I-isoelectronic sequence using both the dual laser produced plasma technique (at DCU) to produce photoabsorption spectra, and the merged ion beam and synchrotron radiation technique (at ASTRID) to measure absolute photoionization cross sections. Profile parameters are compared for the $4s - np$ resonances of Rb^+ and Sr^{2+}. Many new $4p \rightarrow ns$, md transitions are identified with the aid of Hartree-Fock calculations, and consistent quantum defects are observed for the various ns and md Rydberg series. Absolute single and double photoionization cross sections recorded in the $3d$ region for Rb^+ and Sr^{2+} ions show preferential decay via double photoionization. This is only the second report where both the DLP technique and the merged beam technique have been used simultaneously to record photoionization spectra, and the advantages of both techniques (i.e. better resolution in the case of DLP and values for absolute photoionization cross sections in the case of the merged beam technique) are highlighted.

I. INTRODUCTION

There have been numerous systematic investigations of the photoionization of rare gas atoms [1] which were chosen for their simple spherically symmetric closed shell ground state configuration. However the photoionization process was found to be affected by strong electron correlations and this departure from independent electron behaviour resulted in complex excited electronic configuration states and decay dynamics. Dual plasma experiments [2–5], which can be performed on almost any element in any ion stage, have been an important source of experimental data on photoabsorption or photoionization of ions and continue to be an intriguing source of interesting and unusual systems. Measurement of the absolute photoionization cross section of ions with rare gas electronic structures by other methods was inhibited experimentally by the difficulty in generating a stable dense beam of ions in the ground or a selected excited state and the lack of a high flux, high spectral purity tuneable light source. The first measurements of the absolute photoionization cross section of ions (the cross section for the $p \rightarrow d$ resonances in singly ionized Ca, Sr and Ba) were performed on the Daresbury synchrotron radiation source (SRS) by Lyon *et al.* [6–8]. Since this pioneering work, much progress has been made in providing an intense light source which can be used in a merged beam set up at synchrotron facilities worldwide, such as the Photon Factory in Japan, the ASTRID storage ring at the University of Aarhus in Denmark, SPring-8 facility in Japan, the Advanced Light Source at Berkeley, USA, the Super-ACO in France and in the near future at SOLEIL in France. The reader is referred to [9] for a comprehensive review of experimental progress on photoionization of atomic ions.

Experimental data on rare gas-like isoelectronic sequences is invaluable for many reasons, e.g., (i) to track the evolution of atomic dynamics with increasing nuclear charge and ionization, (ii) from a theoretical perspective, the data provide a testing ground for the many atomic codes used to predict atomic and ionic properties and to investigate the interplay between many-body electron-electron correlations and relativistic effects along each isoelectronic sequence, and (iii) measured photoexcitation and absolute photoionization cross sections are vital for correct modelling of stellar atmospheres [10].

The purpose of this paper is to investigate quantitative changes of the $4s - np$, $4p \rightarrow nd$, ms and $3d$-photoionization processes for the Kr I-isoelectronic sequence by measuring the absolute single and double photoionization cross sections for Rb^+ and Sr^{2+} ions, and to make qualitative comparisons with previous studies performed using the dual laser produced plasma technique. The two methods are complementary; the DLP technique has access to many more ion charge states, and is excellent in providing measurements of a high spectral quality over a wide energy range. The merged beam technique provides absolute data directly comparable with sophisticated calculations such as the R-matrix method, and is more selective in determining the charge of the parent species. However both methods suffer from the unwanted presence of metastable species, and this remains a major problem for both techniques. We note that a combination of DLP and synchrotron data has only taken place

once before [11]; in that case, DLP data and relative photoion data were analyzed simultaneously. We summarize in what follows the status concerning what is known from previous work on the corresponding spectra (and where appropriate, related ions) which will help to bring the current paper into context.

The $3s$-subshell photoabsorption spectra of the Ar-isoelectronic sequence was measured by van Kampen *et al.* [12], followed by the absolute photoionization measurements of Kjeldsen *et al.* [13]. These measurements gave rise to further systematic theoretical studies of the evolution of the photoionization cross section from Ar to K^+ to Ca^{2+} [14]. Configuration interaction between single and double electron excited states along the sequence resulted in dramatic and unexpected (for a closed shell atomic system) changes in the $3s - np$ resonance profiles ranging from window resonances in Ar to almost symmetric absorption lines in Ca^{2+}. Neogi *et al.* [15] provided a study of the homologous $4s - np$ resonances of the Kr I-like isoelectronic sequence in the next row of the periodic table. The greater nuclear field experienced by the np-Rydberg electron induces a coupling between the direct and correlative $4s - np$ transition amplitudes resulting again in a drastic change in the $4s - np$ resonances from Kr to Rb^+ to Sr^{2+}. A follow-up to this work (with an upgraded DLP system) was performed on Y^{3+} by Yeates *et al.* [16]. It was found that the $4s - 5p$ resonance drops below the $4p$ ionization threshold so that the first autoionizing member of the $4s - np$ photoionization resonance series becomes $4s - 6p$. Also, whereas the first such series member in Rb^+ and Sr^{2+} appears as a window resonance, in Y^{3+} it switches to a normal, slightly asymmetric absorption peak. Concerning our measurements on the $4s$ subshell excitations we present absolute photoionization cross sections for the $4s - np$ resonances in Rb^+ ($n = 5, 6$) and Sr^{2+} ($n = 5$). Comparisons are made between resonance profile parameters [17] determined in this work and those obtained using the dual laser produced plasma (DLP) technique, and theoretical cross sections computed within the framework of the configuration interaction Pauli-Fock approach presented in [15].

In relation to measurements on $4p$-subshell spectra, Epstein, Reader and Ekberg performed the first elaborate series of emission experiments on the Kr I isoelectronic sequence from Rb II to Mo VII [18]. Using a sliding spark light source, a 10.6-m normal incidence and a 5-m grazing incidence spectrograph, they recorded resonance spectra consisting of the five transitions to the $4p^6\,{}^1S_0$ ground state from levels with $J = 1$ in the $4p^54d$ and $5s$ configurations and calculated ionization energies of 27.285 eV for Rb^+ and 42.87 eV for Sr^{2+}. In [19] the energy-level system of Rb^+ was extended to include previously missing levels which resulted in an improved ionization energy for Rb^+ of 27.2898 eV. As part of the current study the photoabsorption spectra and absolute photoionization cross sections in the $4p$ resonance region are presented for Rb^+ and Sr^{2+}. Newly seen resonances

are presented and the energies and classifications of previously identified lines are compared. Finally quantum defect analyses of the Rydberg series are presented where possible.

In order to put measurements on the $3d$-subshell excitations into context it is worth considering $4d$-subshell excitations in the rare earths. One of the first photoionization studies concentrating on the $4d$ resonance region of the Ba, Ba^+ and Ba^{2+} isonuclear sequence was performed by Lucatorto *et al.* [20] using the resonance laser driven ionization (RLDI) method. Dramatic changes in the photoabsorption spectra with increasing ionization were observed—a redistribution of the $4d$ oscillator strength from a broad $4d \rightarrow \epsilon f$ giant resonance to $4d \rightarrow nf$ discrete resonance structure. As the effective charge on the nucleus increases through the removal of the screening effect of the outer $6s$ electrons, the f wavefunction collapses into the core which increases the overlap with the $4d$ wavefunction and the $4d \rightarrow nf$ transitions become visible. Similar experiments were performed on the next member of the Xe isoelectronic series, La^{3+} [21] using the DLP technique, and on the Xe isonuclear sequence up to Xe^{7+} using merged beam photoion yield spectroscopy [22–25]. However these measurements were only on a relative scale and were superseded by the absolute partial and total photoionization data that followed on Xe [26–28] and Ba ions [29]. Absolute measurements made by Anderson *et al.* [30] on Xe^+ and Xe^{2+} revealed the dominant partial cross section is due to double-photoionization process in $Xe^+ \rightarrow Xe^{3+}$, accounting for 90% or more of the total cross section for the giant $4d$ resonance. Similarly for Xe^{2+} most of the giant resonance is due to double-photoionization process in $Xe^{2+} \rightarrow Xe^{4+}$. Systematic studies by Kjeldsen *et al.* on the following isoelectronic and isonuclear sequences I^+ and I^{2+} [31], I^-, Cs^+, Ba^+ and Ba^{2+} [32] led to the following general conclusion: the total oscillator strength over the $4d$ energy region is close to ten for all atoms and ions studied, which means that the $4d$ shell is relatively unperturbed by other shells. In other words, correlations involving the $4d$ shells are relatively minor. To initiate a study that would verify whether the same holds true for the $3d$ subshell of homologous ions and atoms, we measure here the absolute partial cross section for single- and double- photoionization in the $3d$ region of the Kr I-like isoelectronic series, Rb^+ and Sr^{2+}. Previous DLP [33, 34] and ion yield spectra [35–37] only gave relative cross sections.

The paper is arranged as follows; the experimental methods used to obtain data in this work, namely, the DLP and merged ion beam and synchrotron radiation techniques are described briefly in section II, results for (i) the $4s - np$ resonances, (ii) photoabsorption spectra and absolute photoionization cross sections for $4p \rightarrow ns$, md transitions and (iii) absolute partial single and double photoionization cross sections in the $3d$ region are presented and discussed in section III and finally we draw some conclusions in section IV.

II. EXPERIMENT

The dual laser plasma (DLP) technique [38] was used to record the VUV spectra of rubidium and strontium in this experiment. A Nd:YAG laser (~ 0.7 J in 15 ns) was used to create the absorbing (Rb or Sr) plasma of ions, while a second Nd:YAG laser (~ 0.65 J in 15 ns) tightly focussed onto a tungsten target was used to create the backlighting EUV continuum plasma. In [39] a novel technique of taking a suitable composite or salt target and obtaining the photoabsorption spectra of its constituent elements was applied successfully to obtain the photoabsorption spectra of neutral, singly and doubly ionized bromine using compressed pellets of KBr and CsBr. The technique is successful as long as both constituents of the target do not have transitions occurring in energy range of interest. Here as in [15] compressed rubidium chloride crystal pellets were used. Optimization of absorption due to a particular ionic species was achieved by variation of the time delay between the generation of the absorbing and continuum emitting plasmas and of the position of the absorbing plasma with respect to the optic axis. The optimum time and position for recording Rb$^+$ ion spectra were found to be 400 ns and 1 mm while 150 ns and 1.5 mm gave the purest Sr^{2+} spectra. Once these times and positions had been established they were fixed for the remainder of the experiment irrespective of the detector position on the Rowland circle. This ensures similar plasma conditions for each spectrum which was recorded photoelectrically with a McPherson 2.2-m grazing incidence vacuum spectrograph fitted with an image intensified microchannel plate assembly coupled to a photodiode array detector [38]. The spectra were calibrated against known emission lines of aluminium and the system has a variable instrumental resolution of 1000 or better, dependent on the photon energy range used.

The absolute photoionization cross section measurements were performed in a merged-beam layout which is described in detail by Kjeldsen *et al.* [13, 40]. The interaction between the ions and photons was obtained by merging a beam of Rb$^+$ or Sr^{2+} ions, of energy 2 keV multiplied by the ion charge, with a synchrotron radiation beam over an interaction length of 50 cm, and the absolute single- and double-photoionization cross sections were determined from the photoionization yield of the multiply charged ions. The experiments were performed at the undulator beam line at the 580 MeV storage ring ASTRID at the University of Aarhus. The photon flux was typically $\sim 10^{12}$ photons s^{-1}/0.1% bandwidth and was detected by a calibrated Al$_2$O$_3$ photodiode. The energy resolution was measured to be ~ 40 meV in the $4s - np$ region, ~ 40 meV in the $4p$ region and ~ 730 meV and ~ 1100 meV in the $3d$ region for Rb$^+$ and Sr^{2+} respectively. The photon-energy scale was calibrated using autoionization resonances in He (~ 60 eV), Ne (~ 47 eV) and Kr (~ 90 eV), which were observed in a noble gas ionization chamber. The reference energies were obtained from Domke *et al.* [41], Codling *et al.* [42] and King *et*

al. [43].

The Rb$^+$ and Sr^{2+} ions were produced (from RbCl powder and pure strontium respectively) in a 10 GHz all permanent magnet ECR ion source [44] developed by CEA in Grenoble and used previously at the storage ring SuperACO [22, 29, 44, 45]. The absolute photoionization cross sections were determined from the yield of the various product ions, the current and the velocity of the primary beam, the photodiode current, the interaction length and the effective beam size, together with the detector and photodiode efficiencies. A more detailed description is available in [13, 40]. The photodiode efficiency, which is the main contributor to the total uncertainty, was obtained with the use of a noble gas ionization chamber containing $10 - 100$ mTorr Ne, and using the photoabsorption cross section [46]. Higher order radiation was not significant partly due to the use of Al ($45 - 70$ eV) and Si ($70 - 85$ eV) foils. The absolute cross sections presented are expected to have an uncertainty of $\sim 15\%$.

III. RESULTS AND DISCUSSION

A. $4s - np$ resonances

The absolute photoionization cross sections for the $4s \rightarrow 5p$ and $4s \rightarrow 6p$ Rydberg resonances are presented in Fig. 1 along with the photoabsorption spectra [15]. In the case of photoionization, the spectral profile function σ, for an isolated resonance is given by [17, 47],

$$\sigma = \sigma_0 \left[1 - \rho^2 + \rho^2 \frac{(q + \epsilon)^2}{1 + \epsilon^2} \right] \qquad (1)$$

where $\epsilon = (E - E_r)/(\Gamma/2)$ is the reduced photon energy, E is the incident photon energy, Γ is the resonance width and E_r is the resonance energy position. The Fano parameters ρ and q describe the strength and shape of the resonance respectively. The $4p$ continuum was assumed to decrease linearly with photon energy in the region around the resonances. It has been observed in previous DLP experiments that the profile widths and q-values of Fano-Beutler resonances depend on the absorbance, with optically thin spectra providing best values [48]. For this reason the widths presented in [15] were reduced by 30% and the q-values were increased by $\sim 10\%$. The upper limit on the instrumental resolution for the DLP experiment was ~ 35 meV and ~ 47 meV for Rb$^+$ and Sr^{2+} respectively and ~ 40 meV and ~ 50 meV for the merged beam experiment.

In [15] the $4s - 5p$ photoionization cross sections of Rb$^+$ and Sr^{2+} were calculated within the framework of the configuration interaction Pauli-Fock approach. With reference to Fig. 4 of that paper a qualitative comparison (between the theoretical and experimental absolute cross sections) of the shape and strength of these resonances can be made. In the case of Rb$^+$ the overall

shape of the resonances is in good agreement. However the calculated cross section seems to overestimate the background continuum for example at 35 eV, $\sigma \sim 17$ Mb whereas $\sigma \sim 12.5$ Mb in the absolute cross section measurement. Likewise for Sr^{2+}, while the overall shape of the resonances is in good agreement again the continuum background is overestimated i.e. at 46 eV the calculated cross section $\sigma \sim 8$ Mb and the measured absolute value is $\sigma \sim 7$ Mb.

Table I gives the resonance profile parameters calculated from a fit to eqn. 1 of the absolute cross sections and the photoabsorption cross sections. The spectral resolutions in the two experiments are similar and the data shown in Fig. 1 are in good agreement, once the DLP data have been normalised to the merged beam data. In Table I there are clearly discrepancies in the Γ values for Rb^+ and Sr^{2+} in the case of the $4s - 5p$ resonances; in the case of Rb^+ the values calculated using the two different methods for the DLP data lie on either side of the merged beam value. This indicates that the DLP data do not have a well defined zero in the cross section, as can also be seen from the different values obtained for ρ^2. In the case of Sr^{2+} the DLP data give lower values then the merged beam method for Γ, but the values obtained for ρ^2 are in good agreement throughout. This perhaps indicates that the DLP experimental resolution was superior in this case.

Also presented in Fig. 1 is the $4s - 6p$ resonance observed in Rb^+ only and a comparison with the DLP experiment. The resonance profile was not fitted in the original work [15] but has been fitted here for comparison with the absolute cross section data, using the corrections for the DLP data defined in the first paragraph of this section. The agreement is very satisfactory.

B. $4p - ns, md$ region

Discrete features in the $4p$-photoionization spectra were assigned using the HXR (Hartree plus exchange plus relativistic corrections) of the Cowan code [49]. To compensate for the effect of missing configurations, the Slater parameters F^k, G^k and the configuration parameter R^k were fixed at 85% of the *ab initio* values while the spin-orbit parameter was left unchanged. Transitions from the ground state $3d^{10}4s^24p^6 \, {}^1S_0$ of Rb^+ and Sr^{2+} were identified by performing configuration interaction calculations using the following basis set: $3d^{10}4s^24p^5ns, md$ ($5 \leq n \leq 19$, $4 \leq m \leq 18$). Table II and Table III show the calculated and observed term energies, gf-values, previously known emission lines [19] and where possible, calculated quantum defects (δ). The JJ coupling scheme was favoured over the LS coupling scheme due to the strong spin-orbit mixing of the levels. Synthetic spectra were produced by convolving the calculated oscillator strengths for each transition with an instrumental function of width 0.03 eV followed by normalization to the experimental spectrum. It must be noted that while the
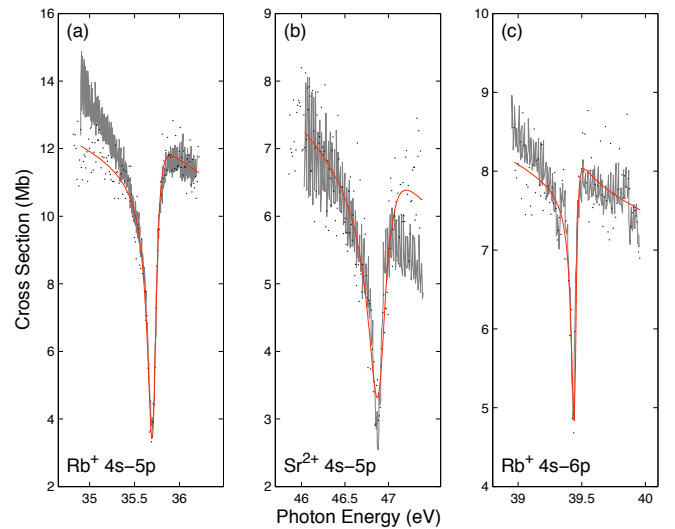

FIG. 1: The experimental absolute single photoionization cross sections for (a) the $4s \rightarrow 5p$ Rydberg resonance of Rb^+, (b) the $4s \rightarrow 5p$ Rydberg resonance of Sr^{2+} and (c) the $4s \rightarrow 6p$ Rydberg resonance of Rb^+. Data from the dual laser produced plasma (black), absolute single- photoionization (black dot) and Fano fit (red) are presented.

TABLE I: Measured profile parameters of $4s - np$ resonances of Rb^+ and Sr^{2+}.

profile parameter	Rb^+ $4s \rightarrow 5p$		
E_r (eV)	35.708 [a]	35.71 ± 0.02 [b]	35.714 [c]
Γ (eV)	0.117 [a]	0.09 ± 0.03 [b]	0.143 [c]
q	0.255 [a]	0.24 ± 0.06 [b]	0.267 [c]
ρ^2	0.40 [a]	0.40 ± 0.10 [b]	0.277 [c]
profile parameter	Sr^{2+} $4s \rightarrow 5p$		
E_r (eV)	46.91 [a]	46.89 ± 0.03 [b]	46.889 [c]
Γ (eV)	0.247 [a]	0.08 ± 0.03 [b]	0.116 [c]
q	0.268 [a]	0.28 ± 0.07 [b]	0.266 [c]
ρ^2	0.22 [a]	0.22 ± 0.05 [b]	0.22 [c]
profile parameter	Rb^+ $4s \rightarrow 6p$		
E_r (eV)	39.442 [a]		39.436 [c]
Γ (eV)	0.045 [a]		0.044 [c]
q	0.291 [a]		0.1955 [c]
ρ^2	0.28 [a]		0.28 [c]

[a] denotes values obtained from fitting the absolute cross section data.

[b] denotes values quoted in [15] for photoabsorption data.

[c] denotes values obtained from fitting the photoabsorption data [15] using the corrections to Γ and q described in the text.

energies in the synthetic spectra are usually quite accurate, the relative intensities cannot be compared quantitatively with the absolute cross section measurements and are presented as a qualitative guide only.

Fig. 2 shows the $4p$-photoabsorption spectrum, the absolute 4p-photoionization cross section and the synthetic

spectrum for Rb$^+$. As noted in section I Reader [19] established the ionization energy of Rb$^+$ to be 27.2898 $\pm$ 0.0001 eV, the ^{2}P$_{\frac{3}{2}}$ series limit of Rb^{2+} with the ^{2}P$_{\frac{1}{2}}$ series limit lying 0.91433 eV above this [18]. The most intense features are due to the $4p \rightarrow nd$ transitions which is quite complicated below the ^{2}P$_{\frac{3}{2}}$ limit. Although good agreement is obtained between lines recorded here and previously identified lines [19], a complete quantum defect analysis was not possible. Above the ionization threshold a clear Rydberg series of $4p \rightarrow nd$ transitions converging on the ^{2}P$_{\frac{1}{2}}$ limit is observed both in the DLP and merged beam experiments. Autoionization calculations were not performed however as the calculated ionization energy (27.497 eV) for Rb^{2+} does not coincide with the actual ionization energy. A quantum defect analysis (presented in Table II) gave acceptable values for $n = 9$ to $n = 15$. However there was some difficulty in determining the peak energies as most of this Rydberg series consists of a blend of a number of md and ns transitions, the ns transitions being too weak to be prominent to any observable degree in the synthetic spectra. The md energies were chosen to be the centre of the first Gaussian profile encountered on increasing energy (as is expected md followed by less intense ns).

TABLE II: Observed and calculated energies and gf-values for the $3d^{10}4s^24p^6 \rightarrow 3d^{10}4s^24p^5nd,\ ms$ transition array of Rb$^+$. The final state JJ coupling of the $3d^9$ core is denoted in brackets by J_{core}, J_{nl}

Upper state	E$_{exp}$ (eV)	E$_{emis}$ (eV)	E$_{calc}$ (eV)	gf-value	δ
$6d(\frac{3}{2},\frac{5}{2})$	24.93	24.929 [a]	24.9313	0.53	
$8d(\frac{3}{2},\frac{5}{2})$	25.77	25.77 [a]	25.7530	0.24	
$8d(\frac{3}{2},\frac{5}{2})$	26.11	26.1090 [a]	26.0542	0.22	
$11d(\frac{3}{2},\frac{5}{2})$	26.37	26.5976 [a]	26.5270	0.08	3.31
$7d(\frac{3}{2},\frac{5}{2})$	26.50		26.6342	0.08	
$12d(\frac{3}{2},\frac{5}{2})$	26.60		26.7194	0.06	3.12
$13d(\frac{3}{2},\frac{5}{2})$	26.72		26.7845	0.04	3.20
$9d(\frac{1}{2},\frac{3}{2})$	27.00		27.1055	0.22	2.27
$10d(\frac{1}{2},\frac{3}{2})$	27.31		27.3099	0.28	2.22
$11d(\frac{1}{2},\frac{3}{2})$	27.50		27.4695	0.22	2.21
$12d(\frac{1}{2},\frac{3}{2})$	27.63		27.5900	0.17	2.23
$13d(\frac{1}{2},\frac{3}{2})$	27.74		27.6814	0.13	2.22
$14d(\frac{1}{2},\frac{3}{2})$	27.82		27.7519	0.10	2.04
$15d(\frac{1}{2},\frac{3}{2})$	27.89		27.8072	0.08	1.92
$16d(\frac{1}{2},\frac{3}{2})$	27.95		27.8515	0.06	1.34

calculated energies are shifted by -0.015 eV. [a] assignments in this work have been made using the jj coupling scheme and vary slightly from the original assignments made in the J_1l coupling scheme (for details of previous assignments see [19]).

FIG. 2: The experimental absolute photoionization cross section for Rb$^+$ in the region of $4p \rightarrow ns$, md excitations. (black) DLP, (blue) absolute single- photoionization spectrum and (red) synthetic spectrum shifted by -0.015 eV.

The $4p$-photoabsorption spectrum, the absolute $4p$-photoionization cross section and the synthetic spectrum for Sr^{2+} are shown in Fig. 3. The ionization energy of Sr^{2+} is 42.87 eV [18], the ^{2}P$_{\frac{3}{2}}$ series limit of Sr^{3+}, and the ^{2}P$_{\frac{1}{2}}$ series limit lies at 1.2061 eV higher [50]. Numerous nd and ms energy levels are classified in table III, with the results of the quantum defect analysis proving to be more consistent for the ms levels. Above the ionization threshold one observes one or two possible resonances in the absolute photoionization cross section. These are not reproduced in the photoabsorption spectrum but are re-produced in the synthetic spectrum. Overall agreement between experiment and theory is good, in particular the energy positions. In the case of the continuum cross sections, we are aware of one calculation relevant to this work [51], but it is difficult to make a direct comparison since data specifically for Rb$^+$ and Sr^{2+} were not presented. However, the indication in that paper was that the continuum cross section should lie between 20 and 50 Mb, in broad agreement with our results.

Contributions from metastable states were observed in the photoabsorption spectrum, the closest lying metastable level to the ground state being $4s^24p^55p$ with a calculated average energy of 28.388 eV. To estimate the contribution from these a separate calculation was performed using the following basis set to account for these metastable contributions, $4s^24p^55p \rightarrow 4p^45pns,\ md$ where $5 \leq n \leq 8$ and $4 \leq m \leq 8$. The synthetic spectrum was calculated in the usual way, i.e., the resulting oscillator strengths were convolved with a Gaussian instrument function of width 0.045 eV and superimposed on the ground state spectrum shown in Fig. 3. Note that this spectrum had to be scaled by a factor of 100 to bring it in line with the experimental spectra, which means that even a small amount of this state being populated could be problematic for the merged beam measurements. However, judging from the data shown in Figs. 2, 3 and 4, where it can be seen that the cross section is close to zero just below the threshold for ionization, the contribution from metastable levels to the

merged beam data seemed negligible and our conclusion is that, within the uncertainty given above, the absolute data are reliable.
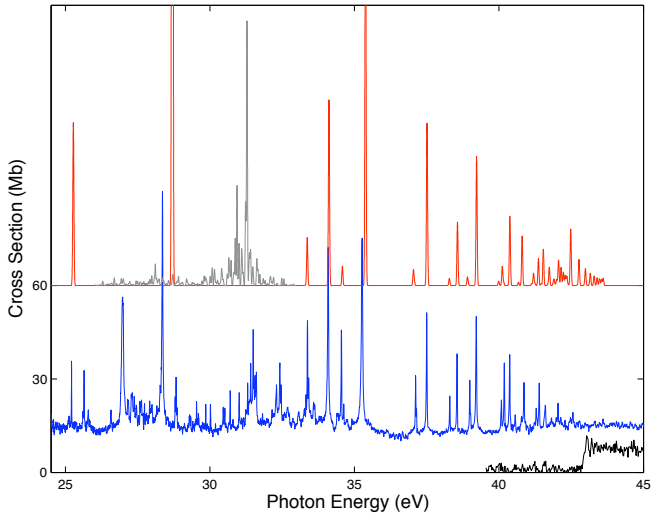

FIG. 3: The experimental absolute photoionization cross section for Sr^{2+} in the region of $4p \rightarrow ns, md$ excitations. (blue) DLP, (black) absolute single- photoionization spectrum, (red) synthetic spectrum and (grey) synthetic metastable spectrum ($\div 100$).

C. $3d$ region

The experimental photoionization cross sections for Rb^+ and Sr^{2+} in the $3d$ region are shown in Fig. 4. The $3d^{10}4s^24p^6 \rightarrow 3d^94s^24p^6np$ transitions have been recorded previously using the DLP technique for Rb^+ and Sr^{2+} [33, 34], which offers better resolution ($\sim$ 200 meV) than is possible with the merged beam experiment ($\sim$ 730 meV and $\sim$ 1100 meV respectively) in this photon energy range. As was the case for the Xe^+ ion the dominant process is double- photoionization, i.e., $Rb^+ \rightarrow Rb^{3+}$ and $Sr^{2+} \rightarrow Sr^{4+}$.

Double photoionization cannot be explained within the framework of a single particle model such as the Hartree-Fock method used here and so as a visual aid and following the work of [36], Fig. 5 shows Grotrian diagrams for the possible decay schemes in both single and double photoionization. Known energy levels and ionization potentials (I.P.) were taken from the following sources: Rb^+ 27.2898 ± 0.0001 eV [19], Rb^{2+} 39.0 ± 0.3 eV [18], Rb^{3+} 52.198 ± 0.248 eV [52], Sr^{2+} 42.87 [18] and Sr^{3+} 56.3 ± 0.2 eV [50]. Unknown energy levels and the Sr^{4+} ionization potential (estimated to be $\sim$ 115.5 eV) were obtained from *ab initio* calculations performed using the HXR (Hartree plus exchange plus relativistic effects) mode of the Cowan code [49]. The single-photoionization cross section arises from either direct photoionization to the ground state $4s^24p^5$ of Rb^{2+} or by the following al-

TABLE III: Observed and calculated energies and gf-values for the $3d^{10}4s^24p^6 \rightarrow 3d^{10}4s^24p^5nd$, ms transition array of Sr^{2+}. The final state JJ coupling of the $3d^9$ core is denoted in brackets by J_{core}, J_{nl}

Upper state	E_{exp} (eV)	E_{emis} (eV)	E_{calc} (eV)	gf-value	δ
$5s(\frac{1}{2},\frac{1}{2})$	25.21	25.211 [a]	25.2724	0.36	2.45
$6s(\frac{1}{2},\frac{1}{2})$	34.55	34.555 [a]	34.5811	0.04	2.42
$7s(\frac{1}{2},\frac{1}{2})$	38.30		38.2829	0.02	2.40
$4d(\frac{3}{2},\frac{5}{2})$	28.35	28.356 [a]	28.6967	5.02	1.10
$5d(\frac{3}{2},\frac{5}{2})$	34.09	34.110 [a]	34.1169	0.41	1.27
$6d(\frac{3}{2},\frac{5}{2})$	37.50	37.496 [a]	37.5097	0.36	1.38
$7d(\frac{3}{2},\frac{5}{2})$	39.22	39.222 [a]	39.2244	0.28	1.21
$8d(\frac{3}{2},\frac{5}{2})$	40.18		40.1148	0.04	1.25
$9d(\frac{3}{2},\frac{5}{2})$	40.86		40.8007	0.11	1.19
$10d(\frac{3}{2},\frac{5}{2})$	41.29		41.1960	0.03	1.21
$11d(\frac{3}{2},\frac{5}{2})$	41.60		41.5336	0.08	1.17
$12d(\frac{3}{2},\frac{5}{2})$	41.81		41.7404	0.04	1.24
$14d(\frac{3}{2},\frac{5}{2})$	42.04		42.0606	0.06	1.27
$15d(\frac{3}{2},\frac{5}{2})$	42.13		42.1484	0.04	1.83
$16d(\frac{3}{2},\frac{5}{2})$	42.21		42.2275	0.03	2.10
$17d(\frac{3}{2},\frac{5}{2})$	42.28		42.2936	0.02	2.42
$18d(\frac{3}{2},\frac{5}{2})$	42.56		42.3486	0.02	2.62
$6s(\frac{3}{2},\frac{1}{2})$	33.37	33.400 [a]	33.3651	0.11	2.41
$7s(\frac{3}{2},\frac{1}{2})$	37.12		37.0377	0.03	2.39
$8s(\frac{3}{2},\frac{1}{2})$	38.99		38.9078	0.02	2.38
$9s(\frac{3}{2},\frac{1}{2})$	40.08		39.9886	0.01	2.38
$5d(\frac{1}{2},\frac{3}{2})$	35.26	35.261 [a]	35.3812	0.88	1.27
$6d(\frac{1}{2},\frac{3}{2})$	38.55	38.552 [a]	38.5636	0.14	1.29
$7d(\frac{1}{2},\frac{3}{2})$	40.37	40.362 [a]	40.3767	0.15	1.25
$8d(\frac{1}{2},\frac{3}{2})$	41.39		41.3645	0.06	1.25
$6d(\frac{3}{2},\frac{3}{2})$	37.15		37.0689	0.01	

[a] assignments in this work have been made using the jj coupling scheme and vary slightly from the original assignments made in the J_1l coupling scheme (for details of previous assignments see [18]).

lowed Auger decay schemes [53],

$$(3d^94s^24p^6np, mf) \rightarrow Rb^{2+*}(3d^{10}4s^24p^4ns, md) + e_1$$
$$\rightarrow Rb^{2+*}(3d^{10}4s^14p^5ns, md) + e_2$$
$$\rightarrow Rb^{2+*}(3d^{10}4s^04p^6ns, md) + e_3$$

Likewise, double-photoionization can occur via direct photoionization to the ground state $4s^24p^4$ of Rb^{3+} or by the following energetically allowed Auger decay scheme, $(3d^94s^24p^6np, mf) \rightarrow Rb^{3+*}(3d^{10}4s^24p^3ns, md)+2e'$; it has long been known that it is the latter which is responsible for the major part of the d-shell continuum cross section. A similar situation exists for Sr^{2+} as is illustrated in Fig 5. The preferential decay via double-photoionization which accounts for 90% of the total $4d$ cross section in Xe^+ is again observed here for the early members of the Kr-I isoelectronic sequence for the total $3d$ cross section. However comparisons of the $3d$ oscillator strengths can-
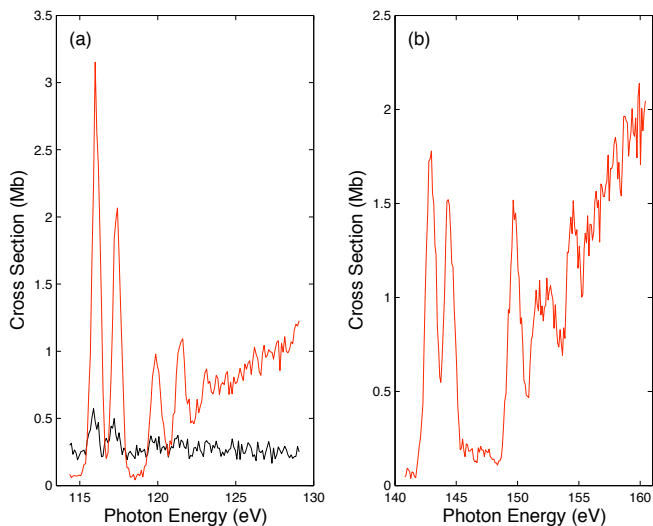
FIG. 4: The experimental absolute photoionization cross section for (a) Rb^+ and (b) Sr^{2+} in the region of $3d$ excitations. Absolute single- photoionization (black) and absolute double-photoionization (red) are presented.

not be made as this would require measurements over a far greater spectral range than is accessible either in the DLP or the merged beam experiments. Indeed with increasing photon energies, resolution becomes poorer and contributions from scattered light can inhibit measurements.

IV. CONCLUSION

$4s-$, $4p-$ and $3d-$ photoionization spectra have been recorded for the first members of the Kr I-isoelectronic sequence, namely Rb^+ and Sr^{2+}. Photoabsorption spectra were recorded using the dual laser produced plasma technique and absolute photoionization cross sections measurements were made using the merged ion beam and synchrotron set up at ASTRID. Good agreement was observed in the case of the fitted profile parameters for the $4s - 5p$ resonances of Rb^+ while the reason for the relatively poor agreement in the case of the resonance width for Sr^{2+} was not clear, but could be due to the poorer resolution of the absolute cross section measurement. Many new $4p \rightarrow ns$, md transitions identified with the aid of Hartree-Fock calculations were presented and consistent quantum defects were observed for the various ns and md Rydberg series in both Rb^+ and Sr^{2+}. In agreement with previous observations [30], partial single- and double- absolute photoionization cross sections recorded in the $3d$ region for Rb^+ and Sr^{2+} ions show preferential decay via double- photoionization. Problems due to contamination from metastable species remain, although in the case of the merged beam data presented here are unlikely to have affected the result. It is hoped that the measurements presented here will encourage further theoretical
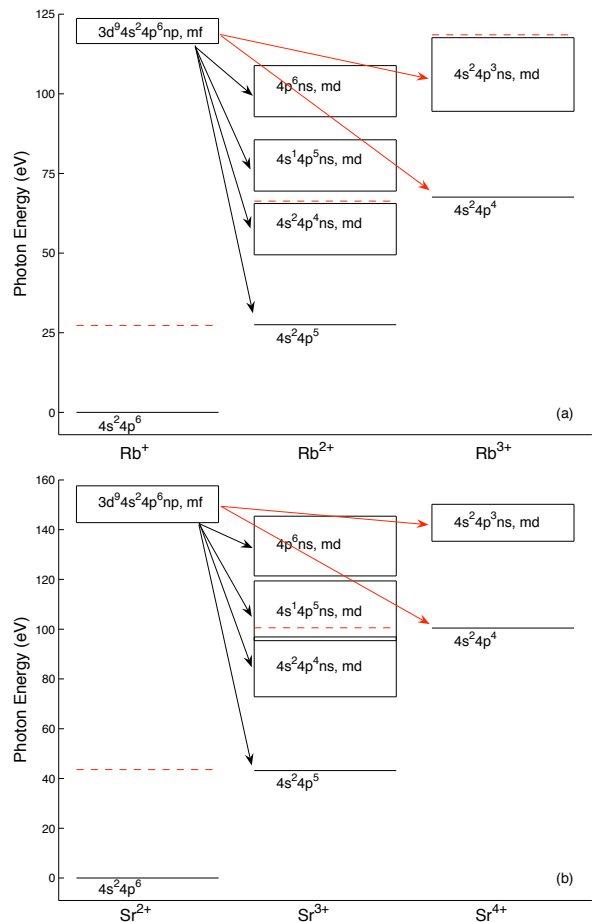

FIG. 5: Grotrian diagrams for the decay of the $3d^{-1}$ excited state of (a) Rb^+ and (b) Sr^{2+}. Single- photoionization decay pathways are indicated by black arrows and double- photoionization decay pathways are indicated by red arrows. The ionization limits are indicated by the red dashed lines.

developments, leading to a greater understanding of the underlying atomic dynamics in the Kr I-isoelectronic sequence.

506008).

[1] V. Schmidt, Rep. Prog. Phys. **55**, 1483 (1992).
[2] A. Carillon, P. Jaeglé, and P. Dhez, Phys. Rev. Lett. **25**, 140 (1970).
[3] J. T. Costello, E. T. Kennedy, J.-P. Mosnier, P. K. Carroll, and G. O'Sullivan, Phys. Scr. **T 34**, 77 (1991).
[4] E. Jannitti, P. Nicolosi, and G. Tondello, Phys. Scr. **41**, 458 (1990).
[5] P. K. Carroll and E. T. Kennedy, Phys. Rev. Lett. **38**, 1068 (1977).
[6] I. C. Lyon, B. Peart, J. B. West, and K. Dolder, J. Phys. B **19**, 4137 (1986).
[7] I. C. Lyon, B. Peart, and K. D. J. B. West, J. Phys. B **20**, 1471 (1987).
[8] I. C. Lyon, B. Peart, and K. Dolder, J. Phys. B **20**, 1925 (1987).
[9] J. B. West, J. Phys. B **34**, R45 (2001).
[10] J. P. Aufdenberg, P. H. Hauschildt, S. N. Shore, and E. Baron, Astrophys. J. **498**, 837 (1998).
[11] P. van Kampen, Ch. Gerth, M. Martins, P. K. Carroll, J. Hirsch, E. T. Kennedy, O. Meighan, J.-P. Mosnier, P. Zimmermann, and J. T. Costello, Phys. Rev. A **61**, 062706 (2000).
[12] P. van Kampen, G. O'Sullivan, V. K. Ivanov, A. N. Ipatov, J. T. Costello, and E. T. Kennedy, Phys. Rev. Lett. **78**, 3082 (1997).
[13] H. Kjeldsen, F. Folkmann, H. Knudsen, M. S. Rasmussen, J. B. West, and T. Andersen, J. Phys. B **32**, 4457 (1999).
[14] B. M. Lagutin, P. V. Demekhin, I. D. Petrov, V. L. Sukhorukov, S. Lauer, H. Liebel, F. Vollweiler, H. Schmoranzer, O. Wilhelmi, G. Mentzel, *et al.*, J. Phys. B **32**, 1795 (1999).
[15] A. Neogi, E. T. Kennedy, J.-P. Mosnier, P. van Kampen, J. T. Costello, G. O'Sullivan, M. W. D. Mansfield, P. V. Demekhin, B. M. Lagutin, and V. L. Sukhorukov, Phys. Rev. A **67**, 042707 (2003).
[16] P. Yeates, E. T. Kennedy, J.-P. Mosnier, P. van Kampen, M. W. D. Mansfield, J. Pedregosa-Gutierrez, J. B. Greenwood, P. V. Demekhin, I. D. Petrov, B. M. Lagutin, *et al.*, J. Phys. B **37**, 4663 (2004).
[17] U. Fano, Phys. Rev. **124**, 1866 (1961).
[18] J. Reader, G. L. Epstein, and J. O. Ekberg, J. Opt. Soc. Am. **62**, 273 (1972).
[19] J. Reader, J. Opt. Soc. Am. **65**, 286 (1975).
[20] T. B. Lucatorto, T. J. McIlrath, J. Sugar, and S. M. Younger, Phys. Rev. Lett. **47**, 1124 (1981).
[21] U. Köble, L. Kiernan, J. T. Costello, J. P. Mosnier, E. T. Kennedy, V. K. Ivanov, V. A. Kupchenko, and M. S. Shendrik, Phys. Rev. Lett. **78**, 2188 (1995).
[22] J. M. Bizau, J.-M. Esteva, D. Cubaynes, F. J. Wuilleumier, C. Blancard, A. C. L. Fontaine, C. Couillaud, J. Lachkar, R. Marmoret, C. Rémond, *et al.*, Phys. Rev. Lett. **84**, 435 (2000).
[23] M. Sano, Y. Itoh, T. Koizumi, T. M. Kojima, S. D. Kravis, M. Oura, T. Sekioka, N. Watanabe, Y. Awaya, and F. Koike, J. Phys. B **29**, 5305 (1996).
[24] N. Watanabe, Y. Awaya, A. Fijino, Y. Itoh, M. Kitajima, T. M. Kojima, M. Oura, R. Okuma, M. Sano, *et al.*, J. Phys. B **31**, 4137 (1998).
[25] T. Koizumi, Y. Awaya, A. Fujima, Y. Itoh, M. Katajima, M. Kojima, , M. Oura, R. Okima, M. Sano, *et al.*, Phys. Scr. **T 71**, 131 (1998).
[26] E. D. Emmons, A. Aguilar, M. F. Gharaibeh, S. W. J. Scully, R. A. Phaneuf, A. L. D. Kilcoyne, A. S. Schlachter, I. Álvarez, C. Cisneros, and G. Hinojosa, Phys. Rev. A **71**, 042704 (2005).
[27] J.-M. Bizau, C. Blancard, D. Cubaynes, F. Folkmann, J. P. Champeaux, J. L. Lemaire, and F. J. Wuilleumier, Phys. Rev. A **73**, 022718 (2006).
[28] A. Aguilar, J. D. Gillaspy, G. F. Gribakin, R. A. Phaneuf, M. F. Gharaibeh, M. G. Kozlov, J. D. Bozek, and F. J. Wuilleumier, Phys. Rev. A **73**, 032717 (2006).
[29] J.-M. Bizau, D. Cubaynes, J.-M. Esteva, F. J. Wuilleumier, C. Blancard, J. P. Champeaux, A. Compant La Fontaine, C. Couillaud, M. R., and C. R. et al, Phys. Rev. Lett. **87**, 273002 (2001).
[30] P. Andersen, T. Andersen, F. Folkmann, V. K. Ivanov, H. Kjeldsen, and J. B. West, J. Phys. B **34**, 2009 (2001).
[31] H. Kjeldsen, P. Andersen, F. F. H. Knudsen, B. Kristensen, J. B. West, and T. Andersen, Phys. Rev. A **62**, 020702(R) (2000).
[32] H. Kjeldsen, P. Andersen, F. F. J. E. Hansen, M. Kitajima, and T. Andersen, J. Phys. B **35**, 2845 (2002).
[33] C. McGuinness, G. O'Sullivan, P. K. Carroll, D. Audley, and M. W. D. Mansfield, Phys. Rev. A **51**, 2053 (1995).
[34] A. Neogi, E. T. Kennedy, J.-P. Mosnier, P. van Kampen, J. T. Costello, C. McGuinness, and G. O'Sullivan, J. Phys. B **34**, L656 (2001).
[35] T. Koizumi, T. Hayaishi, Y. Itikawa, T. Nagata, Y. Sato, and A. Yagishita, J. Phys. B **20**, 5393 (1987).
[36] T. Koizumi, T. Hayaishi, Y. Itikawa, Y. Itoh, T. Matsuo, T. Nagata, Y. Sato, E. Shigemasa, A. Yagishita, and M. Yoshino, J. Phys. B **23**, 403 (1990).
[37] Y. Itoh, T. Koizuma, Y. Awaya, S. D. Kravis, M. Oura, M. Sano, T. Sekioka, and F. Koike, J. Phys. B **28**, 4733 (1995).
[38] E. T. Kennedy, J. T. Costello, J.-P. Mosnier, A. A. Cafolla, M. Collins, L. Kiernan, U. Köble, M. H. Sayyad, M. Shaw, and B. F. Sonntag, Opt. Eng. **33**, 3984 (1994).
[39] A. Cummings and G. O'Sullivan, Phys. Rev. A **54**, 323 (1996).
[40] H. Kjeldsen, F. Folkmann, B. Kristensen, J. B. West, and J. E. Hansen, Nucl. Instrum. Methods Phys. Res. B **234**, 349 (2005).
[41] M. Domke, K. Schulz, G. Remmers, G. Kaindl, and D. Wintgen, Phys. Rev. A **53**, 1424 (1996).
[42] K. Codling, R. P. Madden, and D. L. Ederer, Phys. Rev. **155**, 26 (1967).
[43] G. C. King, M. Tronc, F. H. Read, and R. C. Bradfor, J. Phys. B **10**, 2479 (1976).
[44] J.-M. Bizau, E. Bouisset, C. Blancard, J. P. Champeaux, C. la Fontaine A., C. Couillaud, D. Cubaynes, D. Hitz, C. Vinsot, and F. J. Wuilleumier, Nucl. Instrum. Meth. B **205**, 290 (2003).
[45] J.-P. Champeaux, J.-M. Bizau, D. Cubaynes, C. Blancard, S. N. Nahar, D. Hitz, J. Bruneau, and F. J. Wuilleu-

mier, ApJS **148**, 583 (2003).

[46] G. V. Marr and J. B. West, At. Data Nucl. Data Tables **18**, 497 (1976).

[47] U. Fano and J. W. Cooper, Phys. Rev. **137**, A1364 (1965).

[48] A. Gray, *Ph. D. thesis* (Dublin City University, 1999).

[49] R. D. Cowan, *The Theory of Atomic Structure and Spectra* (University of California Press, Berkeley, CA, 1981).

[50] J. E. Hansen and W. Persson, Phys. Scr. **13**, 166 (1976).

[51] A. Msezane R. F. Reilman S. T. Manson J. R. Swanson and L. Armstrong, Phys. Rev. A **15**, 668 (1977).

[52] W. Persson and C.-G. Wahlström, Phys. Scr. **31**, 487 (1985).

[53] H. Aksela, R. Lakanen, S. Aksela, O. -P. Sairanen, A. Yagashita, M. Meyer, T. Prescher, E. von Raven, M. Richter, and B. Sonntag, Phys. Rev. A **38**, 3395 (1988).